Coupled-channels calculations of ^{16}O + ^{16}O fusion

H. Esbensen

Physics Division, Argonne National Laboratory, Argonne, Illinois 60439, USA
(Received 17 March 2008; published 27 May 2008)

Fusion data for ^{16}O + ^{16}O are analyzed by coupled-channels calculations. It is shown that the calculated cross sections are sensitive to the couplings to the 2^+ and 3^- excitation channels even at low energies, where these channels are closed. The sensitivity to the ion-ion potential is investigated by applying a conventional Woods-Saxon potential and the M3Y+repulsion potential, consisting of the M3Y double-folding potential and a repulsive term that simulates the effect of the nuclear incompressibility. The best overall fit to the data is obtained with a M3Y+repulsion potential that produces a shallow potential in the entrance channel. The stepwise increase in measured fusion cross sections at high energies is also consistent with such a shallow potential. The steps are correlated with overcoming the barriers for the angular momenta $L = 12, 14, 16,$ and 18. To improve the fit to the low-energy data requires a shallower potential and this causes a even stronger hindrance of fusion at low energies. It is therefore difficult, based on the existing fusion data, to make an accurate extrapolation to energies that are of interest to astrophysics.

I. INTRODUCTION

A major challenge in nuclear astrophysics is to measure the cross sections for radiative capture and fusion reactions with high precision and down to very low energies. Another challenge is to develop models that can reproduce the existing data and be used with confidence to extrapolate the cross sections to the energies that are of interest to astrophysics. Examples of reactions where these challenges exist are the low-energy fusion of ^{12}C + ^{12}C, ^{12}C + ^{16}O, and ^{16}O + ^{16}O. It was recently suggested [1] that the fusion rates that have been used in the past for these reactions should be reduced because of a hindrance phenomenon, and the implications for stellar burning and nucleosynthesis were investigated in Ref. [2]. The fusion hindrance has been observed experimentally at extreme sub-barrier energies in many medium-heavy systems [3] but it has not yet been observed convincingly in lighter systems. It is therefore of interest to study the possible evidence for such a phenomenon in light systems.

The theoretical description of light-ion fusion reactions, for example, of the ^{16}O + ^{16}O fusion data [4], is often limited to optical model calculations. An exception is the study by Reinhard *et al.* [5] in which the ion-ion potential for ^{16}O + ^{16}O was derived from an adiabatic TDHF calculation, and the fusion cross sections that were calculated have served as guidance for the extrapolation to low energies. The purpose of this work is to use the coupled-channels method to analyze the ^{16}O + ^{16}O fusion data of Ref. [4] to investigate the influence of the couplings to the 2^+ and 3^- excitations of the reacting nuclei and to see whether the fusion hindrance phenomenon is likely to exist in such a light system.

The coupled-channels method has been used in numerous analyses of the fusion data for medium-heavy nuclei. It has been very successful in many cases in reproducing the data at energies near and slightly below the Coulomb barrier, typically down to 0.1 or 0.01 mb. Thus it has been possible to generate the large enhancement that is needed to fit the

data at sub-barrier energies by including couplings to surface excitation modes, primarily to the low-lying 2^+ and 3^- states, and to two-phonon and mutual excitations of these states (see, for example, the review article Ref. [6] and the proceedings Refs. [7,8]). In some cases it is necessary to include couplings to transfer channels (see Refs. [7,8]).

The definition of fusion in the coupled-channels approach is usually based on ingoing wave boundary conditions (IWBC). They are imposed at a distance somewhere inside the Coulomb barrier, for example, at the minimum of the pocket in the entrance channel potential. However, a short-ranged imaginary potential has also been used to simulate the fusion. The two ways of defining the fusion give essentially the same result in most cases. This supports the view that the fusion is primarily sensitive to the description in the vicinity of and outside the Coulomb barrier, and the empirical proximity-type Woods-Saxon potential [9], which is based on extensive analyses of elastic-scattering data and also on the M3Y double-folding potential, has served as a very realistic interaction in coupled-channels calculations.

The above view of the fusion process has been challenged by the discovery of the fusion hindrance at extreme sub-barrier energies. Because the hindrance sets in at a rather high excitation energy of the compound nucleus, it was suggested early that it had to be an entrance channel phenomenon [10]. It was shown in Ref. [11] that the hindrance could be explained by adjusting the ion-ion potential at small distances between the reacting nuclei so it produced a shallow potential in the entrance channel. In contrast, the empirical interaction of Ref. [9] produces a relative deep pocket, and the M3Y double-folding potential is unphysical because it produces a pocket that is much deeper than the ground-state energy of the compound nucleus. It was proposed in Ref. [11] that the new low-energy fusion data offer the opportunity to investigate the radial dependence of the ion-ion potential at short distances.

We have shown that a shallow potential can be constructed by correcting the M3Y double-folding potential with

a repulsive term that simulates the effect of the nuclear compressibility [12]. Thus we were able to explain successfully the fusion data for ^{64}Ni + ^{64}Ni [13], ^{28}Si + ^{64}Ni [14], and ^{16}O + ^{208}Pb [15], ranging in cross sections from 20 nb to 1 b. It is therefore of interest to apply this type of potential in the analysis of the ^{16}O + ^{16}O fusion data to see how it will affect the extrapolation to extreme sub-barrier energies.

With an increased sensitivity (at extreme sub-barrier energies) to the potential at small distances between the fusing nuclei, one should also be concerned about the validity of the basic assumptions in the coupled-channels approach, namely that the structure input is that of the isolated nuclei. For strongly overlapping nuclei, the modes of excitations may be better described in terms of excitations of the compound nucleus. Unfortunately, it is very difficult in the coupled-channels approach to develop a model that includes a realistic transition from a dinuclear description to a compound nucleus description. Some justification for the coupled-channels method can be found, for example, in calculations that are based on the two-center Hartree-Fock method. Thus, in the case of ^{16}O + ^{16}O, Zint and Mosel found that the individual shell structures of the two ^{16}O nuclei survive up to a remarkable degree of overlap [16]. Moreover, the ion-ion potential they determined gives a very shallow potential in the entrance channel, in qualitative agreement with the empirical findings from the analysis of elastic-scattering data [17] and also, as we shall see, from the analysis of the fusion data.

II. COUPLED-CHANNELS DESCRIPTION

The fusion cross sections for the oxygen isotopes are somewhat exceptional in the sense that they are rather structureless [4], whereas fusion data for ^{12}C + ^{12}C [18] and ^{12}C + ^{16}O [19] contain very rich structures or resonances. Because the coupled-channels calculations presented here produce rather smooth and structureless cross sections at low energies, the investigations will be restricted to the fusion of ^{16}O + ^{16}O.

The basic assumptions and ingredients in the coupled-channels description of fusion reactions are summarized below. The structure input for the 2^+ and 3^- states in ^{16}O [20,21] is shown in Table I. The channels for the two excited states in ^{16}O become closed when the center-of-mass (c.m.) energy is less than the excitation energy, $E_x \approx 6$–7 MeV. The asymptotic boundary condition for the radial wave function $u_{nL}(r)$ in an open, inelastic channel n with angular momentum L is the outgoing Coulomb wave,

$$u_{nL}(r) \propto O_L(q_n r) = G_L(\eta_n, q_n r) + i F_L(\eta_n, q_n r),$$

TABLE I. Properties of the 2^+ and 3^- states in ^{16}O. The B values and Coulomb coupling strengths are from Ref. [20]. The nuclear couplings are from α scattering [21].

Nucleus	λ^π	E_x (MeV)	$B(E\lambda)$ (W.u.)	β_λ^C	$(\frac{\beta R}{\sqrt{4\pi}})_C$ (fm)	$(\frac{\beta R}{\sqrt{4\pi}})_N$ (fm)
^{16}O	2^+	6.92	3.1(1)	0.35	0.30	0.27
	3^-	6.13	13.5(7)	0.72	0.61	0.40

$$\text{for } r \to \infty, \tag{1}$$

where $\hbar q_n$ is the asymptotic relative momentum and $\eta_n = Z_1 Z_2 e^2/(\hbar v)$ is the Sommerfeld parameter for channel n. The outgoing wave is here expressed in terms of the regular and irregular Coulomb wave functions F_L and G_L, respectively. For a closed channel the condition (1) is replaced by

$$u_{nL}(r) \propto W_{-\eta_n, L+1/2}(2q_n r), \tag{2}$$

where $W_{-\eta, L+1/2}(z)$ is the Whittaker function.

The coupled equations are solved in the so-called rotating frame approximation. A detailed discussion of the coupled-equations in this approximation can be found, for example, in Ref. [22]. The boundary conditions that are used at short distances are the ingoing-wave boundary conditions (IWBC), which are imposed at the location of the minimum of the pocket in the entrance channel, and the fusion cross section is determined by the ingoing flux. This model works quite well at energies that are near and below the Coulomb barrier.

It is a common problem that one cannot always reproduce the fusion data at extreme sub-barrier energies and at energies far above the Coulomb barrier by using exactly the same model assumptions in the two energy regimes. It has been suggested that the problem can be solved by considering the effect of decoherence [23] but calculations that demonstrate this point were not carried out. The solution we have used [15] is to supplement the IWBC at energies far above the Coulomb barrier with a weak imaginary potential that acts near the minimum of the pocket in the entrance channel. The need for such an imaginary potential at high energies may reflect the influence of an increasing number of reaction channels, which cannot be considered explicitly in a practical calculation.

A. Standard Woods-Saxon potential

The real part of the ion-ion potential is commonly parametrized as a Woods-Saxon potential,

$$V(r) = \frac{V_0}{1 + \exp[(r - R_{\text{pot}})/a]}, \tag{3}$$

and the proximity type potential discussed in Ref. [9] [Eq. (40)] will be used below. The results of coupled-channels calculations that are based on this potential will be compared to data and to calculations that use the M3Y+repulsion potential [12]. These two types of potentials are basically identical at large radial distances between the reacting nuclei, and they produce essentially the same Coulomb barrier height. They differ at short distances, as will be shown in the next section. The Woods-Saxon potential produces a relatively deep pocket in the entrance channel potential, whereas the M3Y+repulsion potential can be adjusted to produce a shallow pocket and a thicker Coulomb barrier. The latter two features help explain the hindrance of fusion [12–15], which has been observed in many heavy-ion systems at extreme sub-barrier energies. The issue here is whether an analysis of the fusion data for ^{16}O + ^{16}O will show a sensitivity to the potential at short distances.

B. Fusion cross sections

The fusion cross sections for ^{16}O $+$ ^{16}O that were measured by Thomas *et al.* [4] are compared in Fig. 1 to coupled-channels calculations and to the no-coupling limit, i.e., a one-dimensional barrier penetration calculation. Both calculations are based on the standard proximity type, Woods-Saxon potential [9]. The uncertainty in the data was taken from the published figures, except at center-of-mass energies larger than 8 MeV, where an (arbitrary) uncertainty of 5% was adopted, because it was not possible to read the small experimental uncertainty. Earlier measurements do exist, see, for example, Refs. [24–26], but they are not shown here.

The proximity type, Woods-Saxon potential [9], in which the radius has been adjusted to provide the best fit to the ^{16}O $+$ ^{16}O fusion data [4], has the following parameters: $V_0 = -42.14$ MeV, $R_{\rm pot} = 6.083$ fm, and $a = 0.602$ fm. The solid curve (CCC) in Fig. 1 is the coupled-channels result one obtains with this potential and it has a $\chi^2/N = 1.5$. The dashed curve shows the no-coupling limit (NOC) one obtains with the same potential. The fit to the data in the no-coupling limit can be improved by adjusting the radius of the potential. The best fit is achieved for $R_{\rm pot} = 6.133$ fm and has a $\chi^2/N = 4.2$. This is much larger than the $\chi^2/N = 1.5$ obtained in the coupled-channels calculation and shows that the couplings to the 2^+ and 3^- states do play a significant role.

It may be seen in Fig. 1 that the measured cross sections fall off faster with decreasing energy than predicted by the coupled-channels calculation at the lowest energies. This is a signature of the onset of the fusion hindrance phenomenon discussed earlier. The hindrance will be explored further in the following sections.

III. THE M3Y+REPULSION POTENTIAL

The calculation of the M3Y+repulsion potential is described in Ref. [12] but some of the essential features are summarized here. First, one calculates the M3Y double-folding potential (including the exchange term). This requires

as input the proton and neutron densities of projectile and target. The densities of protons and neutrons were assumed to be identical for ^{16}O and the form of density was assumed to be a Fermi function with radius $R = 2.5$ fm and diffuseness $a = 0.52$ fm. The radius was adjusted so that the measured RMS charge radius of 2.737(8) fm [27] was reproduced.

The repulsive term associated with the nuclear incompressibility is also obtained from the double-folding procedure using a repulsive effective NN interaction of the form $V_{\rm rep}\delta(\mathbf{r})$. The density that is used in connection with the repulsive term has the same radius as the ordinary densities mentioned above but the diffuseness $a_{\rm rep}$ is chosen differently. Thus there are two parameters in the calculation of the repulsive interaction, the strength $V_{\rm rep}$ and the diffuseness $a_{\rm rep}$ of the density. They are constrained, as explained in Ref. [12], so the total nuclear interaction for completely overlapping nuclei, $U_N(r = 0)$, is consistent with the equation of state $\epsilon(\rho)$ at normal nuclear matter density ρ and $\epsilon(2\rho)$ at twice the nuclear matter density. This condition was expressed in Ref. [12] by the relation

$$U_N(r = 0) = 2A_a[\epsilon(2\rho) - \epsilon(\rho)] \approx \frac{A_a}{9}K. \qquad (4)$$

Here A_a is the mass number of the smaller nucleus, so the equation expresses the change in energy one has by embedding the smaller nucleus inside the larger. The last approximation relates this change in energy to the nuclear incompressibility, $K = 9\rho^2[d^2\epsilon(\rho)/d\rho^2]$.

The entrance channel potential obtained from the M3Y+repulsion potential is illustrated in Fig. 2 for a range of values of the diffuseness parameter $a_{\rm rep}$. The strength of the repulsive interaction $V_{\rm rep}$ was adjusted in each case to produce the nuclear incompressibility $K = 234$ MeV. This is the value that has been obtained from the Thomas-Fermi equation of state for symmetric nuclear matter [28]. The smallest value of $a_{\rm rep}$, which is 0.3 fm, produces a pocket that is as deep as the energy of the compound nucleus ^{32}S. The
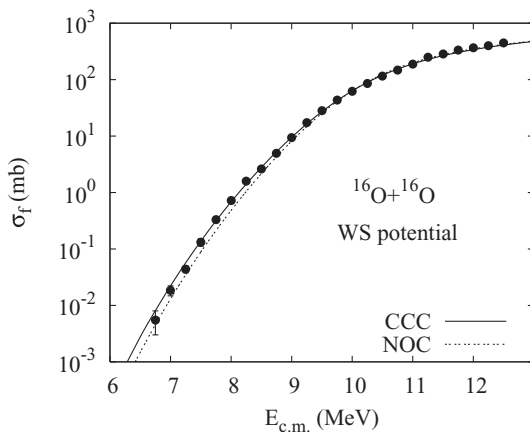

FIG. 1. The fusion cross sections for ^{16}O $+$ ^{16}O measured by Thomas *et al.* [4] are compared to coupled-channels calculations (CCC) and to the no-coupling limit (NOC). Both calculations are based on the Woods-Saxon potential described in the text.
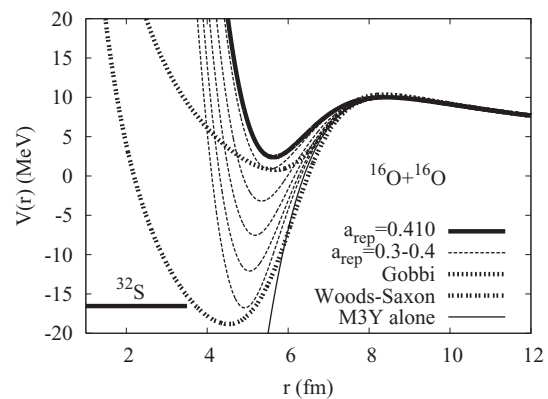

FIG. 2. The M3Y+repulsion entrance-channel potential is shown for $a_{\rm rep} = 0.41$ fm, and for $a_{\rm rep} = 0.3$–0.4 fm in steps of 0.025 fm. The Woods-Saxon, the Gobbi [17], and the pure M3Y entrance channel potentials are also shown, and the energy of the compound nucleus ^{32}S is indicated.

largest value, $a_{rep} = 0.41$ fm, produces a pocket at 2.4 MeV and has a Coulomb barrier of 10.01 MeV.

The thin solid curve in Fig. 2 is the entrance channel potential one obtains with the pure M3Y potential (including the exchange term). It has an unrealistic and extremely deep pocket, which is far below the energy of the compound nucleus. The entrance potential, which is based on the Woods-Saxon potential discussed in the previous section, is shown by the lower thick dashed curve. It is slightly deeper than the ground state of the compound nucleus and it has a Coulomb barrier of 10.10 MeV.

Finally, the upper thick dashed curve in Fig. 2 is the shallow Gobbi potential [17], which, by the way, is in surprisingly good agreement with the potential obtained in the two-center Hartree-Fock calculation of Ref. [16]. It is seen that the M3Y+repulsion and Gobbi potentials have almost the same depth but the thickness of the Coulomb barrier is different. It turns out that the thicker barrier provided by the M3Y+repulsion potential gives a much better fit to the fusion data when applied in the coupled-channels calculations.

A. Fusion cross sections

The thick solid curve in Fig. 2, which is based on the diffuseness parameter $a_{rep} = 0.41$ fm, is the entrance channel potential that provides the best fit to the fusion data in the coupled-channels calculations. The calculated cross section is shown by the solid curve in Fig. 3 and it has a $\chi^2/N = 1.3$. The quality of the fit is only slightly better than what was obtained in the previous section using the standard Woods-Saxon potential. The slight improvement is difficult to see but it is achieved mainly at the lowest energies.

The χ^2/N is shown in Fig. 4 as function of the diffuseness parameter a_{rep}. There are two minima, one at a small value, $a_{rep} \approx 0.325$, and one at $a_{rep} = 0.41$ fm, which is by far the best solution. It is of interest to compare a_{rep} to the values that have been used for other systems. Thus for the $^{64}Ni + ^{64}Ni$ system we obtained the best fit to the data for $a_{rep} = 0.403$ fm [12]. For $^{28}Si + ^{64}Ni$ the value was 0.392 fm [14],

FIG. 4. The χ^2/N obtained from the $^{16}O + ^{16}O$ fusion data [4] and coupled-channels calculations. The χ^2/N is shown as function of the diffuseness parameter a_{rep}, which determines the repulsive term in the M3Y+repulsion potential.

and for the very asymmetric system $^{16}O + ^{208}Pb$ we had to use the smaller value $a_{rep} = 0.35$ fm [15].

The discrepancy with the data is emphasized in Fig. 5 where ratios of the measured and calculated fusion cross sections are shown. The solid circles are the coupled-channels results and the open circles show the results in the no-coupling limit obtained with the same potential, namely the M3Y+repulsion potential with $a_{rep} = 0.41$ fm. The effect of the couplings to the 2^+ and 3^- excitations is to bring the cross-section ratio closer to 1. However, there are still some minor deviations from 1. For example, the ratio of the measurement and the coupled-channels calculation (solid circles) shows a decreasing trend with decreasing energy below 8 MeV and it is less than 1 at the lowest energy point. This is a signature of the experimental fusion hindrance with respect to the coupled-channels calculation.
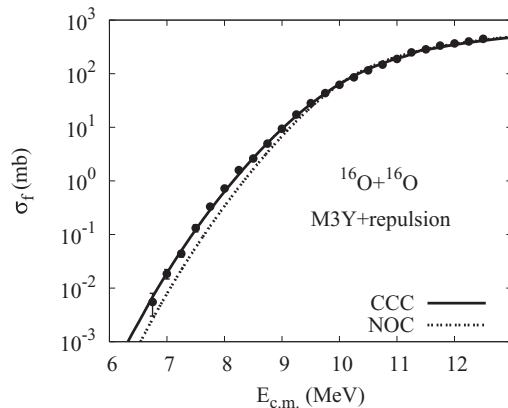

FIG. 3. The fusion data for $^{16}O + ^{16}O$ [4] are compared to coupled-channels calculations (CCC) and to the no-coupling limit (NOC). Both calculations are based on the M3Y+repulsion potential with $a_{rep} = 0.41$ fm.
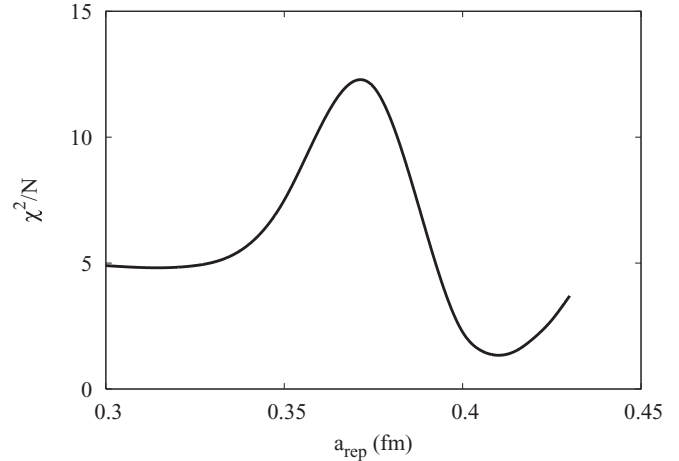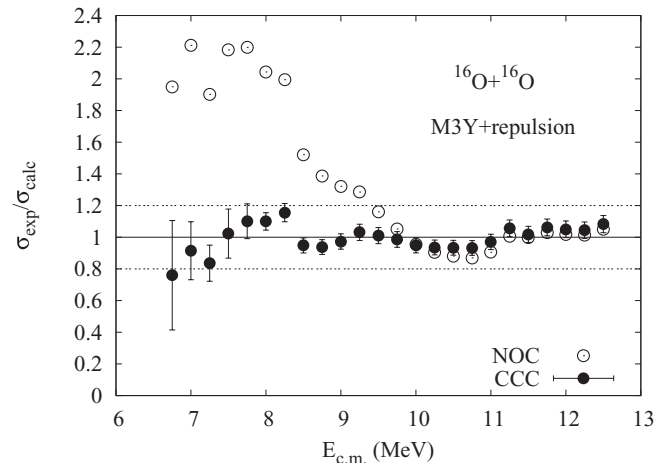

FIG. 5. Ratio of experimental [4] and calculated cross sections shown in Fig. 3.

IV. THE *S* FACTOR AT LOW ENERGIES

It is unfortunate that the quality of the fit of the coupled-channels calculations to the ^{16}O + ^{16}O fusion data is essentially the same whether we use the Woods-Saxon or the M3Y+repulsion potentials. From the empirical knowledge of the fusion hindrance phenomenon [3] one would have expected that the M3Y+repulsion potential would provide a much better description of the low-energy data. However, the improvement is modest. One would need measurements at even lower energies to be able to see a stronger sensitivity to the ion-ion potential at short distances.

A good way to emphasize the low-energy behavior of the measured and calculated fusion cross sections is to plot the *S* factor for fusion defined by

$$S = E_{c.m.}\sigma_f \exp(2\pi\eta), \qquad (5)$$

where η is the Sommerfeld parameter. The experimental *S* factors are compared in Fig. 6 to the two coupled-channels calculations that were discussed earlier. The top dashed curve is based on the Woods-Saxon potential, whereas the solid curve is based on the M3Y+repulsion potential. The latter provides a slightly better fit to the data at the lowest energies but the error bars are large so the overall improvement in terms of a χ^2/N is modest, as discussed in the previous section.

The two coupled-channels calculations shown in Fig. 6 start to deviate as the energy is reduced. The calculation that is based on the M3Y+repulsion potential (the solid curve) develops a maximum near 4 MeV. The reason is that the entrance channel potential has a pocket at 2.4 MeV, and this forces the *S* factor to vanish below that energy when the fusion is determined by IWBC. It is interesting that the value of the *S* factor at 4 MeV (solid curve) is in fair agreement with the prediction of the adiabatic TDHF calculation [5]. However, the *S* factor for fusion obtained in the adiabatic TDHF calculation keeps increasing with decreasing energy [5].

It is not clear *a priori* whether the *S* factor for the fusion of ^{16}O + ^{16}O should develop a maximum at low energy. It
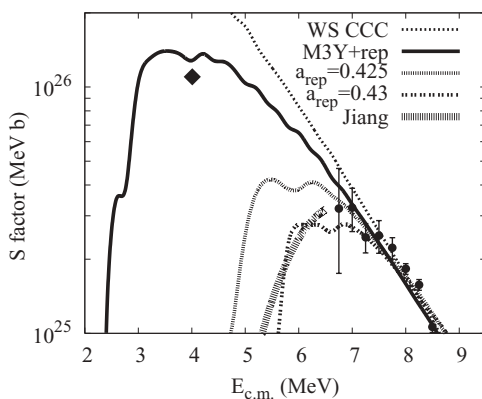

FIG. 6. *S* factors for the coupled-channels calculations shown in Figs. 1 and 3 are compared to the data [4]. Also shown are coupled-channels calculations that are based on shallower potentials, with $a_{rep} = 0.425$ and 0.43 fm, respectively. The diamond is the adiabatic TDHF results [5]. The lowest thick curve is the extrapolation made by Jiang *et al.* [1].

does not have to do that because the ground-state *Q* value for producing ^{32}S is positive. It is only for negative *Q* values one can argue that the *S* factor must have a maximum at some positive center-of-mass energy [3].

There is an alternative extrapolation method [3] that is based on the logarithmic derivative of the energy-weighted fusion cross section,

$$L(E) = \frac{1}{E_{c.m.}\sigma_f} \frac{d(E_{c.m.}\sigma_f)}{dE}. \qquad (6)$$

This quantity has a nearly linear dependence on energy at extreme sub-barrier energies in most of the medium-heavy systems that have been studied experimentally. The linear dependence makes it fairly easy to extrapolate the data to the energy where the *S* factor has a maximum [3].

A better parametrization of $L(E)$ was adopted in Ref. [1]. By considering all of the 50 data points that have been measured below 8.5 MeV [4,24–26] it was concluded that the *S* factor for the fusion of ^{16}O + ^{16}O must have a maximum close to 7 MeV. The extrapolation to lower energies that was obtained in Ref. [1] is shown in Fig. 6 in terms of the *S* factor by the lowest, thick curve. The low-energy fusion cross sections predicted by this extrapolation are even more suppressed than the coupled-channels calculation that is based on the M3Y+repulsion potential.

Apparently, there are certain features of the data that are not reproduced by the coupled-channels calculations presented here. Some indications of that can be seen in the cross-section ratios shown in Fig. 5. For example, the seven lowest data points form an isolated group that is disconnected from the rest above 8.5 MeV. It is not clear what causes the discontinuity; is it a remnant of a resonance or is it an experimental problem? In any case, one can adjust the M3Y+repulsion potential so that the coupled-channels calculations reproduce the the energy dependence of the seven lowest points, i. e., so that the cross-section ratio $\sigma_{exp}/\sigma_{calc}$ becomes a constant. This can be achieved with a diffuseness parameter in the range $a_{rep} = 0.425$–0.43 fm, which produces a pocket in the entrance channel potential in the range of 4.5 to 5.2 MeV. The *S* factors obtained from such calculations are also shown in Fig. 6. The results are in fair agreement with the extrapolation method proposed by Jiang *et al.* [1]. That is not surprising because the latter extrapolation was also based on low-energy data.

Fusion should in principle be allowed down to zero energy because the ground state of the compound nucleus ^{32}S is at a much lower energy (see Fig. 2). To describe the fusion at such low energies would require an extension of the model used here, for example, along the lines proposed in Ref. [29].

V. FUSION AT HIGH ENERGIES

Another way to test the ion-ion potential is to compare to cross sections that have been measured at energies far above the Coulomb barrier. Here the data are often suppressed compared to calculations that are based on a conventional Woods-Saxon potential, with a relatively deep entrance potential [30]. We have previously shown that the shallow entrance channel potential, produced by the M3Y+repulsion potential,
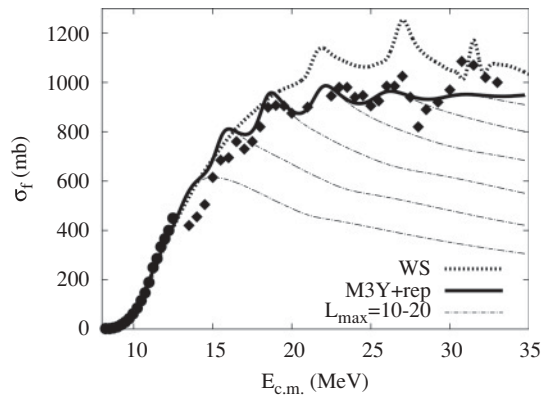
FIG. 7. The measured fusion cross sections for $^{16}\text{O} + ^{16}\text{O}$ (solid circles [4]; diamonds [31]) and coupled-channels calculations that are based on the Woods-Saxon (top dashed) and M3Y+repulsion potential (with $a_{\text{rep}} = 0.41$, solid curve). The thin dashed curves show the dependence on the maximum angular momentum L_{max}. All calculations include a short-range imaginary potential.

gives a better description of the high-energy fusion data for $^{16}\text{O} + ^{208}\text{Pb}$ [15]. However, it was necessary to supplement the nuclear interaction with a weak, short-ranged imaginary potential. It is interesting that the same conclusions apply to to the high-energy fusion of $^{16}\text{O} + ^{16}\text{O}$.

The results of coupled-channels calculations that are based on the M3Y+repulsion potential and a short-ranged imaginary potential that acts near the minimum of the potential pocket are compared in Fig. 7 to the data of Tserruya *et al.* [31]. The data exhibit an oscillatory or stepwise increasing behavior that was also seen in the earlier data by Kolata *et al.* [32]. This behavior is qualitatively reproduced by the calculation (solid curve). The stepwise increase in the calculated cross section is correlated with overcoming the potential barriers for $L = 12, 14, 16,$ and 18. This can be seen by comparing to the thin dashed curves that show the cross sections one obtains by imposing different values of the maximum angular momentum L_{max} in the calculations. Note that only even values of L are considered for a symmetric system.

The coupled-channels calculations that are based on the deep Woods-Saxon potential are shown by the upper thick dashed curve in Fig. 7. It is seen that the data are suppressed compared to this calculation and that the stepwise behavior sets in at a higher energy and a higher angular momentum ($L = 16$ to be precise, compared to $L = 12$ in the solid curve.) Thus the high-energy $^{16}\text{O} + ^{16}\text{O}$ fusion data show a clear preference for the shallow potential produced by the M3Y+repulsion interaction.

The analysis of the elastic-scattering data for $^{16}\text{O} + ^{16}\text{O}$ by Gobbi *et al.* [17] also revealed the need for a shallow potential. The potential they obtained is illustrated by the upper thick dashed curve in Fig. 2. The minimum of the pocket is in this case at 0.78 MeV, which is slightly deeper that the 2.4 MeV pocket produced by the M3Y+repulsion potential (with $a_{\text{rep}} = 0.41$ fm). Thus it appears that both the elastic-scattering data and the high-energy fusion data prefer a shallow pocket in the entrance channel.

It should be mentioned that the Gobbi potential does not provide a good description of the low-energy fusion data by Thomas *et al.* [4], although it has a shallow pocket. The reason is that the Coulomb barrier is not as thick as the one produced by the M3Y+repulsion potential (see Fig. 2.) As a consequence, the fusion data are hindered compared to calculations that are based on the Gobbi potential.

VI. CONCLUSIONS

It has been shown that the calculated fusion cross sections for $^{16}\text{O} + ^{16}\text{O}$ are sensitive to couplings to the 2^+ and 3^- excited states of ^{16}O even at low energies, where the excitation channels are closed. Unfortunately, the overall quality of the fit to the fusion data by Thomas *et al.* [4] is not very sensitive to the ion-ion potential at short distances between the reacting nuclei. It is only at the very lowest energies that there is a preference for a shallow potential in the entrance channel.

The potential that gives the best fit to the fusion data by Thomas *et al.* [4] is the M3Y double-folding potential that has been corrected for the effect of the nuclear incompressibility. This M3Y potential is calculated with a density that is consistent with the measured charge radius of ^{16}O, and it produces a very realistic height of the Coulomb barrier. The repulsive interaction that simulates the effect of the nuclear incompressibility is calculated with parameters (the nuclear incompressibility and a diffuseness parameter) that are similar to those that have been used previously to reproduce the low-energy fusion data for medium-heavy systems.

The fusion cross sections obtained in coupled-channels calculations are in fairly good agreement with measurements at high energies when the calculations are based on the shallow M3Y+repulsion potential. In particular, the oscillatory or stepwise increasing behavior is reproduced very well, whereas the calculations that are based on the deeper Woods-Saxon do not reproduce the data. The evidence for a shallow entrance channel potential is corroborated by the empirical optical potential for the elastic-scattering obtained by Gobbi *et al.* [17].

The S factor obtained in the coupled-channels calculations that give the best fit to the data by Thomas *et al.* has a maximum at a center-of-mass energy near 4 MeV. The value of the S factor at this energy is close to the value that was predicted more than 20 years ago in an adiabatic TDHF calculation. However, if the potential is adjusted to improve the fit only to the low-energy data, one obtains an even stronger hindrance of fusion at lower energies. This is in qualitative agreement with the empirical extrapolation proposed recently by Jiang *et al.* [1]. To confirm the hindrance experimentally one would have to measure the fusion cross section down to an energy of 5–6 MeV.

[1] C. L. Jiang, K. E. Rehm, B. B. Back, and R. V. F. Janssens, Phys. Rev. C **75**, 015803 (2007).

[2] L. R. Gasques, E. F. Brown, A. Chieffi, C. L. Jiang, M. Limongi, C. Rolfs, M. Wiescher, and D. G. Yakovlev, Phys. Rev. C **76**, 035802 (2007).

[3] C. L. Jiang, B. B. Back, H. Esbensen, R. V. F. Janssens, and K. E. Rehm, Phys. Rev. C **73**, 014613 (2006).

[4] J. Thomas, Y. T. Chen, S. Hinds, D. Meredith, and M. Olson, Phys. Rev. C **33**, 1679 (1986).

[5] P. G. Reinhard, J. Friedrich, K. Goeke, F. Grümmer, and D. H. E. Gross, Phys. Rev. C **30**, 878 (1984).

[6] A. B. Balantekin and N. Takigawa, Rev. Mod. Phys. **70**, 77 (1998).

[7] *Proceedings of the International Conference FUSION03: From a Tunneling Nuclear Microscope to Nuclear Processes in Matter*, edited by N. Takigawa *et al.*, Prog. Theor. Phys. Suppl. 154 (2004).

[8] *Proceedings of the International Conference FUSION06: Reaction Mechanisms and Nuclear Structure at the Coulomb Barrier*, edited by L. Corradi *et al.*, AIP Conf. Proc. vol. 853 (2006).

[9] R. A. Broglia and A. Winther, *Frontiers in Physics Lecture Notes Series: Heavy-Ion Reactions* (Addison-Wesley, Redwood City, CA, 1991), Vol. 84.

[10] C. L. Jiang *et al.*, Phys. Rev. Lett. **89**, 052701 (2002).

[11] C. H. Dasso and G. Pollarolo, Phys. Rev. C **68**, 054604 (2003).

[12] Ş. Mişicu and H. Esbensen, Phys. Rev. C **75**, 034606 (2007).

[13] Ş. Mişicu and H. Esbensen, Phys. Rev. Lett. **96**, 112701 (2006).

[14] C. L. Jiang *et al.*, Phys. Lett. **B640**, 18 (2006).

[15] H. Esbensen and Ş. Mişicu, Phys. Rev. C **76**, 054609 (2007).

[16] P. G. Zint and U. Mosel, Phys. Rev. C **14**, 1488 (1976).

[17] A. Gobbi, R. Wieland, L. Chua, D. Shapira, and D. A. Bromley, Phys. Rev. C **7**, 30 (1973).

[18] E. F. Aguilera *et al.*, Phys. Rev. C **73**, 064601 (2006).

[19] J. R. Patterson, B. N. Nagorcka, G. D. Symons, and W. M. Zuk, Nucl. Phys. **A165**, 545 (1971).

[20] Evaluated Nuclear Structure Data Files (ENSDF), National Nuclear Data Center, Brookhaven National Laboratory, http://www.nndc.bnl.gov/

[21] K. T. Knöpfle *et al.*, Phys. Rev. Lett. **35**, 779 (1975).

[22] H. Esbensen, Prog. Theor. Phys. Suppl. **154**, 11 (2004).

[23] M. Dasgupta, D. J. Hinde, A. Diaz-Torres, B. Bouriquet, C. I. Low, G. J. Milburn, and J. O. Newton, Phys. Rev. Lett. **99**, 192701 (2007).

[24] H. Spinka and H. Winkler, Nucl. Phys. **A233**, 456 (1974).

[25] G. Hulke, C. Rolfs, and H. P. Trautvetter, Z. Phys. A **297**, 161 (1980).

[26] S.-C. Wu and C. A. Barnes, Nucl. Phys. **A422**, 373 (1984).

[27] H. de Vries, C. W. de Jager, and C. de Vries, At. Data Nucl. Data Tables **36**, 495 (1987).

[28] W. D. Myers and W. J. Świątecki, Phys. Rev. C **57**, 3020 (1998).

[29] T. Ichikawa, K. Hagino, and A. Iwamoto, Phys. Rev. C **75**, 057603 (2007).

[30] J. O. Newton *et al.*, Phys. Lett. **B586**, 219 (2004).

[31] I. Tserruya, Y. Eisen, D. Pelte, A. Gavron, H. Oeschler, D. Berndt, and H. L. Harney, Phys. Rev. C **18**, 1688 (1978).

[32] J. J. Kolata, R. C. Fuller, R. M. Freeman, F. Haas, B. Heusch, and A. Gallmann, Phys. Rev. C **16**, 891 (1977).